


RESEARCH ARTICLE

Tropical rainfall predictions from multiple seasonal forecast systems

Adam A. Scaife^{1,2}  | Laura Ferranti³ | Oscar Alves⁴ | Panos Athanasiadis⁵ | Johanna Baehr⁶ | Michel Dequé⁷ | Tina Dippe⁸ | Nick Dunstone¹ | David Fereday¹ | Richard G. Gudgel⁹ | Richard J. Greatbatch⁸ | Leon Hermanson¹ | Yukiko Imada¹⁰ | Shipra Jain¹¹ | Arun Kumar¹² | Craig MacLachlan¹ | William Merryfield¹³ | Wolfgang A. Müller¹⁴ | Hong-Li Ren¹⁵ | Doug Smith¹ | Yuhei Takaya¹⁰ | Gabriel Vecchi¹⁶ | Xiaosong Yang^{9,17}

¹Met Office Hadley Centre, Met Office, Exeter, UK

²College of Engineering, Mathematics and Physical Sciences, University of Exeter, Exeter, UK

³European Centre for Medium-Range Weather Forecast (ECMWF), Reading, UK

⁴Bureau of Meteorology, Melbourne, Australia

⁵Centro Euro-Mediterraneo sui Cambiamenti Climatici, Bologna, Italy

⁶Center for Earth System Research and Sustainability, Institute of Oceanography, Universität Hamburg, Hamburg, Germany

⁷Centre National de Recherches Météorologiques (UMR 3589), Toulouse, France

⁸GEOMAR Helmholtz Centre for Ocean Research Kiel Düsternbrooker Weg 20, Kiel, Germany

⁹Geophysical Fluid Dynamics Laboratory, National Oceanic and Atmospheric Administration, Princeton, New Jersey

¹⁰Climate Research Department, Meteorological Research Institute, Japan Meteorological Agency, Tsukuba, Japan

¹¹National Centre for Medium Range Weather Forecasting (NCMRWF), Ministry of Earth Sciences, Noida, India

¹²NOAA/National Centers for Environmental Prediction, College Park, Maryland

¹³Canadian Centre for Climate Modelling and Analysis, Environment and Climate Change Canada, University of Victoria, Victoria, British Columbia, Canada

¹⁴Max Planck Institute for Meteorology, Hamburg, Germany

¹⁵Laboratory for Climate Studies, National Climate Center, China Meteorological Administration, Beijing, China

¹⁶Geosciences Department and Princeton Environmental Institute, Princeton University, Princeton, New Jersey

¹⁷University Corporation for Atmospheric Research, Boulder, Colorado

Correspondence

Adam A. Scaife, Met Office Hadley Centre, Met Office, Fitz Roy Road, Exeter EX1 3PB, UK.
Email: adam.scaife@metoffice.gov.uk

Funding information

Joint DECC/Defra Met Office Hadley Centre Climate Programme, Grant/Award Number: GA01101; UK-China Research & Innovation Partnership Fund through the Met Office Climate Science for Service Partnership (CSSP) China as part of the Newton Fund; European Union 7th Framework Programme (FP7 2007–2013), Grant/Award Number: 603521; German Ministry of Education and Science, Grant/Award Numbers: 03G0837A, 01LP1517D; Universität Hamburg; Cluster of Excellence CliSAP, Grant/Award Number: EXC177; Ministry of Education and Research, Grant/Award Number: 01LP1519A

We quantify seasonal prediction skill of tropical winter rainfall in 14 climate forecast systems. High levels of seasonal prediction skill exist for year-to-year rainfall variability in all tropical ocean basins. The tropical East Pacific is the most skilful region, with very high correlation scores, and the tropical West Pacific is also highly skilful. Predictions of tropical Atlantic and Indian Ocean rainfall show lower but statistically significant scores.

We compare prediction skill (measured against observed variability) with model predictability (using single forecasts as surrogate observations). Model predictability matches prediction skill in some regions but it is generally greater, especially over the Indian Ocean. We also find significant inter-basin connections in both observed and predicted rainfall. Teleconnections between basins due to El Niño–Southern Oscillation (ENSO) appear to be reproduced in multi-model predictions and are responsible for much of the prediction skill. They also explain the

This is an open access article under the terms of the Creative Commons Attribution License, which permits use, distribution and reproduction in any medium, provided the original work is properly cited.

© 2018 Crown copyright, Met Office Weather © 2018 Royal Meteorological Society This article is published with the permission of the Controller of HMSO and the Queen's Printer for Scotland

relative magnitude of inter-annual variability, the relative magnitude of predictable rainfall signals and the ranking of prediction skill across different basins.

These seasonal tropical rainfall predictions exhibit a severe wet bias, often in excess of 20% of mean rainfall. However, we find little direct relationship between bias and prediction skill. Our results suggest that future prediction systems would be best improved through better model representation of inter-basin rainfall connections as these are strongly related to prediction skill, particularly in the Indian and West Pacific regions. Finally, we show that predictions of tropical rainfall alone can generate highly skilful forecasts of the main modes of extratropical circulation via linear relationships that might provide a useful tool to interpret real-time forecasts.

KEYWORDS

ensemble, ENSO, NAO, PNA, seasonal prediction, tropical rainfall

1 | INTRODUCTION

While significant progress has been made in recent years, there is a limit of around 2 weeks to deterministic weather forecast skill for daily rainfall, and most of the skill falls away by the second week (e.g., Li and Robertson, 2015; Stern and Davidson, 2015). In addition, numerous studies point to limitations of general circulation models in the simulation of rainfall in the Tropics. The poor reproduction of the Madden–Julian Oscillation (e.g., Ahn *et al.*, 2017) and the challenges of accurately parametrizing tropical convection (e.g., Arakawa, 2004) are commonly cited reasons.

Despite these well-known limitations on shorter time-scales, the long-range prediction of seasonal rainfall in the Tropics is highly skilful, and seasonal mean skill scores a few months ahead far exceed the skill of weather forecasts in the extratropics just days ahead (Stockdale *et al.*, 1998; Dequé, 2001; Kumar *et al.*, 2013; Molteni *et al.*, 2015; Scaife *et al.*, 2017). This capability is of great interest for early warning of the risk of tropical drought and flooding (e.g., Dutra *et al.*, 2014; Li *et al.*, 2016). However, we also note that tropical rainfall has an influence on the extratropics via Rossby waves (e.g., Hoskins and Karoly, 1981; Simmons *et al.*, 1983; Li *et al.*, 2014). Recent advances in winter seasonal prediction of extratropical circulation (e.g., Riddle *et al.*, 2013; Kang *et al.*, 2014; Scaife *et al.*, 2014; Yang *et al.*, 2015; Athanasiadis *et al.*, 2017) are strongly linked to these teleconnections from the Tropics (Greatbatch *et al.*, 2012; Molteni *et al.*, 2015; Kumar and Chen, 2017; Scaife *et al.*, 2017) as are some inter-annual (Dunstone *et al.*, 2016) and even decadal variations (Trenberth *et al.*, 2014; Smith *et al.*, 2016) and so our study is focussed on the winter season.

Previous single model studies (Kumar *et al.*, 2013; Molteni *et al.*, 2015) have documented high tropical skill and linear inverse modelling suggests that seasonal forecasts

may already be near the predictability limit in the East Pacific (Newman and Sardeshmukh, 2017). We therefore investigate tropical rainfall predictability in multiple seasonal prediction systems to document the variation of skill across different models and also across different tropical regions (section 3). We also compare the skill in predicting observed rainfall variability with the level of predictability inherent in the models (section 4) and show how well the dominant influence of El Niño–Southern Oscillation (ENSO) and inter-basin connections are reproduced in current prediction systems in section 5. Given that much climate model development is focused on improving the mean state, in section 6 we investigate whether there is a relationship between the magnitude of mean state errors (i.e., forecast drift) and seasonal forecast skill. Finally, in section 7 we show that using tropical rainfall forecasts alone can provide highly skilful predictions of extratropical inter-annual variability in the winter Pacific North American pattern and the North Atlantic Oscillation.

2 | SEASONAL PREDICTION SYSTEMS

We analyse winter (December–January–February) mean predictions of tropical rainfall from 14 seasonal prediction systems over the period 1992/1993 to 2011/2012 where available. These retrospective predictions are all initialized on or close to November 1 and the November data are excluded to prevent contamination from medium range predictability. Brief details and references for further details of each system follow:

U.K. Met Office predictions are from the operational global seasonal prediction system GloSea (Arribas *et al.*, 2011). Data used here are from GloSea5—the fifth generation of this forecast system which has relatively high resolution and uses coupled ocean, sea-ice and land surface model

components (MacLachlan *et al.*, 2015). Ensemble generation is through a combination of lagged start dates and stochastic physics perturbations to produce an ensemble of 24 member forecasts for each winter, initialized around early November, approximately 1 month ahead of winter as described in MacLachlan *et al.* (2015). The atmospheric resolution of the model is 0.83° longitude by 0.55° latitude with 85 quasi-horizontal atmospheric levels and an upper boundary at 85 km. Ocean resolution is 0.25° globally with 75 quasi-horizontal levels.

Canadian Climate Centre models CanCM3 and CanCM4 share the same coupled ocean, land and sea-ice components. The land component is version 2.7 of the Canadian Land Surface Scheme (CLASS). Sea-ice dynamics are governed by cavitating fluid rheology, and thermodynamics by a simple energy balance model. The CanCM3 atmospheric component is CanAM3 (Scinocca *et al.*, 2008), whereas the CanCM4 atmospheric component is CanAM4 (Von Salzen *et al.*, 2013). Upgraded physical parameterizations in CanAM4 include fully prognostic cloud and aerosol schemes, improved radiation schemes and a parameterization of shallow convection. Ten ensemble members are generated for both CanCM3 and CanCM4 using initial conditions from 10 separate simulations constrained by observations. Horizontal resolution in both cases is T63 or about 2.8° . CanAM3 has 31 vertical levels and CanAM4 35 levels, both extending to 1 hPa. Horizontal resolution of the ocean component is approximately 100 km, with 40 vertical levels. Further details are provided in Merryfield *et al.* (2013).

European Centre for Medium Range Weather Forecasting (ECMWF) seasonal forecasts are from ECMWF system 4 (Molteni *et al.*, 2011) with atmospheric model IFS cycle 36r4 coupled to the HTESSEL land surface model and the Nucleus for European Modelling of the Ocean (NEMO) ocean model (Madec, 2008) via the OASIS3 coupler (Valcke, 2013). An ensemble of 15 forecasts was made from November 1 for each winter using stochastic physics perturbations. Ozone is a prognostic variable and is radiatively active. Time-variation of greenhouse gases and solar cycle are specified, although solar variability is not spectrally resolved. Volcanic aerosols are included based on the estimated distribution in the month prior to the start of the forecast, and then follow damped persistence. There is no dynamical sea-ice in this system. For the first 10 days, the forecast persists the initial sea-ice analysis; then there is a transition towards specified ice conditions derived from the previous 5 years. This sea-ice configuration captures the main trend in sea-ice and gives a representation of the uncertainty in sea-ice conditions. The atmospheric model has a spectral truncation T255 (~ 80 km resolution) and 91 levels in the vertical. The ocean model has 42 vertical levels and a horizontal resolution of about 1° in the extratropics with an equatorial refinement to $1/3^\circ$ latitude.

Météo-France predictions are from version 5 of the Meteo-France seasonal forecast system. It is based on the Centre National de Recherches Météorologiques Coupled Model version 5 (CNRM-CM5; Voltaire *et al.*, 2013). The four components of the model are Arpege 6.0 (atmosphere), Surfex 7.3 (continental surfaces), Nemo 3.2 (ocean) and Gelato 5.1 (sea ice). Each forecast ensemble is initialized on November 1 and contains 15 ensemble members generated by stochastic perturbations (Batté and Déqué, 2016). This model also uses coupled, prognostic ozone, in this case initialized from climatology. The atmosphere resolution is TL255 (0.7°) with 91 vertical levels. The ocean resolution is 1° and has 42 vertical levels.

The Centro Euro-Mediterraneo sui Cambiamenti Climatici (CMCC) data used here are from the CMCC Seasonal Prediction System version 1.5 (hereafter referred to as CMCC, Matera *et al.*, 2014), while a general description of the model components is given in Alessandri *et al.* (2010). The CMCC-SPS-v1.5 uses the ECHAM5 atmospheric model coupled to OPA8.2 ocean model and the SILVA land surface model and sea-ice initialized from climatology. The ensemble consists of nine members covering the period 1983–2011 and initialized on November 1 each year using lagged initial conditions. The horizontal resolution in the atmosphere is T63 with 19 vertical levels up to 10 hPa. The ocean resolution is around 2° with 31 vertical levels.

Beijing Climate Centre (BCC) seasonal prediction data are from the BCC/China Meteorological Administration (CMA) operational system 2, which is based on the BCC Climate System Model version 1.1 m (BCC_CSM1.1m; Wu *et al.*, 2013). The BCC Atmospheric GCM is coupled to the BCC Atmosphere and Vegetation Interaction Model version 1.0, the Geophysical Fluid Dynamics Laboratory (GFDL) Modular Ocean Model version 4 (Griffies *et al.*, 2005) and the Sea Ice Simulator (Winton, 2000). Forecasts are initialized for each calendar month from the four-time daily NCEP/NCAR R1 data and the oceanic initial values from ocean temperature of the NCEP Global Oceanic Data Assimilation System (GODAS), using a nudging scheme with timescale of 2 days while sea ice is interactive but not initialized (Liu *et al.*, 2015). The BCC ensemble includes 24 forecast members initialized near the beginning of November: 9 are perturbed by an empirical singular vector (Cheng *et al.*, 2010) and 15 are generated from the lagged average of the atmospheric states on the first 5 days of each month and the ocean states on the first 3 days which are combined to generate 15 further members. The ocean model resolution is 1° with 40 levels and the atmospheric horizontal resolution is T106 with 26 vertical hybrid sigma/pressure levels (Wu *et al.*, 2010).

National Centers for Environmental Prediction (NCEP) data are from the Climate Forecast System version (CFSv2; Saha *et al.*, 2014). CFSv2 is a coupled ocean–atmosphere–land dynamical seasonal prediction system. The oceanic

component is the Geophysical Fluid Dynamics Laboratory Modular Ocean Model version 4 including the sea-ice simulator (MOM4; Griffies *et al.*, 2005). CFSv2 forecasts are initialized from the Climate Forecast System Reanalysis (CFSR; Saha *et al.*, 2010). For CFSv2 forecasts, there is one forecast at 00Z, 06Z, 12Z and 18Z every fifth day of the year and the 12 forecast members from October 18, 23, 28 are used here. The atmospheric component is at horizontal resolution of T126 (~100 km) with 64 vertical levels and the ocean is at 0.25° with 10° of the equator, tapering to 0.5° poleward of 30° latitude.

The Kiel Climate Model (KCM) couples the atmospheric model ECHAM5 (Roeckner *et al.*, 2003) with interactive land surface to the NEMO-based ocean model OPA9 (Madec *et al.*, 1998; Madec, 2008) with coupled LIM2 sea-ice model, using the OASIS3 coupler (Valcke, 2013). For more details see Park *et al.* (2009). An ensemble of nine members was run from November 1 for each winter using the nine different combinations of ocean and atmosphere initial states from three assimilation runs, where the model was run in partially coupled mode to minimize equatorial initialization shock (Ding *et al.*, 2013; Thoma *et al.*, 2015). The ocean and sea-ice components in the assimilation runs were forced with observed wind stress anomalies from ERA-Interim, added to the model's native wind stress climatology. Radiative forcing was constant in time. Here we used the KCM in a coarse resolution: ECHAM5 at T31 with 19 vertical levels, OPA9 with the ORAC2 horizontal grid (roughly 1.3° horizontal resolution, refined to 0.5° at the equator) and 31 vertical levels.

The hindcasts from GFDL were produced from the Forecast-oriented Low Ocean Resolution model (FLOR; Vecchi *et al.*, 2014). The atmosphere and land components of FLOR are taken from the GFDL Coupled Model version 2.5 (CM2.5; Delworth *et al.*, 2012), whereas the ocean and sea-ice components are based on the GFDL Coupled Model version 2.1 (CM2.1; Delworth *et al.*, 2006; Wittenberg *et al.*, 2006). FLOR is an operational seasonal forecast model in the North American Multi-Model Ensemble for seasonal prediction (Kirtman *et al.*, 2014). Twelve-member ensemble forecasts are initialized in November from 1991 to 2012. The initial conditions of the ocean and ice components are from the GFDL ensemble coupled data assimilation (ECDA) system (Zhang *et al.*, 2007; Chang *et al.*, 2013). Initial conditions for the atmosphere and land are from a set of AMIP simulations with time-varying observed SST (Reynolds *et al.*, 2002) and radiative forcing. FLOR has a spatial resolution of ~50 km in the atmosphere and land, ~100 km in the ocean and 32 (50) vertical levels in the atmosphere (ocean). Further details of FLOR and its initialization can be found in Vecchi *et al.* (2014).

The Australian Bureau of Meteorology POAMA seasonal forecast system is based on a coupled ocean-atmosphere model and data assimilation system (Hudson

et al., 2013). The land surface component is a simple bucket model for soil moisture (Manabe and Holloway, 1975) and has three soil levels for temperature (Hudson *et al.*, 2011). The ocean model is the Australian Community Ocean Model version 2 (ACOM2; Schiller *et al.*, 1997; 2002) and is based on the Geophysical Fluid Dynamics Laboratory (GFDL) Modular Ocean Model (MOM version 2). The atmosphere and ocean models are coupled using the Ocean Atmosphere Sea Ice Soil (OASIS) coupling software (Valcke, 2013). Forecasts are initialized from assimilated atmospheric and oceanic states using ocean initial conditions from the POAMA Ensemble Ocean Data Assimilation System (Yin *et al.*, 2011a). Climatological sea-ice is imposed in the simulations and the atmosphere and land initial conditions are taken from the atmosphere-land initialization scheme (Hudson *et al.*, 2011). A 10 member ensemble was initialized on November 1 using a coupled-model breeding scheme (Yin *et al.*, 2011b; Hudson *et al.*, 2013). The atmospheric model has T47 horizontal resolution with 17 vertical levels and the ocean grid resolution is 2° in longitude and 0.5° in latitude at the Equator, increasing to 1.5° near the poles.

The Max-Planck Institute Earth System Model version 1.0 in low resolution (MPI-ESM-LR; Giorgetta *et al.*, 2013) was used to perform an ensemble of hindcasts (Baehr *et al.*, 2015). This configuration consists of the atmospheric component ECHAM6 (Stevens *et al.*, 2013). The ocean component consists of the Max-Planck Institute Ocean Model (MPIOM; Jungclaus *et al.*, 2013). The oceanic and atmospheric components are coupled through the Ocean-Atmosphere-Sea-Ice coupler (Valcke, 2013). The initial conditions are obtained by Newtonian relaxation (“nudging”) of the atmosphere, ocean and sea-ice to ERA-Interim, ORAS4 and NSIDC, respectively (see Baehr *et al.*, 2015 for details). Bred vectors in the oceanic component of the model are used to generate initial perturbations for the ensemble (following Baehr and Piontek, 2013). An ensemble of 10 forecasts was made from November 1. The atmospheric component is spectrally resolved with a truncation at wave-number 63 (~200 km), and with physics represented on a regular Gaussian grid in the horizontal and 47 vertical levels and the ocean model uses a bi-polar grid at nominal 1.5° horizontal resolution.

Japan Meteorological Agency (JMA) predictions are from the operational global seasonal prediction system JMA/MRI-CPS2 (Takaya *et al.*, 2017). The sea-ice component is incorporated in the coupled model. Data analysed here are from a lagged ensemble of 10 member forecasts for each winter that started from initial dates in the second half of October as described in Takaya *et al.* (2017). The model was initialized using the atmosphere and land analysis from the Japanese 55-year Reanalysis (JRA-55; Kobayashi *et al.*, 2015), and ocean and sea-ice analysis from the Multivariate Ocean Variational Estimation/Meteorological Research Institute Community Ocean Model-Global version 2 (MOVE/

MRI.COM-G2; Toyoda *et al.*, 2013). The resolution of the atmospheric component is approximately 110 km with 60 vertical levels with a model top at 0.01 hPa. The oceanic component has 52 vertical levels a horizontal resolution of 1° in longitude and 0.5° in latitude with an equatorial refinement to 0.3°.

The Model for Interdisciplinary Research on Climate (MIROC) seasonal predictions (Imada *et al.*, 2015) are provided by the Atmosphere and Ocean Research Institute (AORI), National Institute for Environmental Studies (NIES), and the Japan Agency for Marine-Earth Science and Technology (JAMSTEC). Data used here are from MIROC version 5 (Watanabe *et al.*, 2010). A lagged ensemble of eight-member forecasts for each winter was initialized around early November. In the initialization process, the observed temperature and salinity anomalies in the ocean were incorporated into the model fields under the 20th century and CMIP5 climate forcing of solar radiation, volcanic forcing, greenhouse gases, ozone, aerosol and land-use change (Tatebe *et al.*, 2012), no sea-ice or land surface observations are used in the initialization. The resolution of the atmospheric component is triangular spectral truncation at total horizontal wave number 85 (T85) with 40 vertical layers. The oceanic component has a horizontal resolution of 1.4° in longitude and 0.9° in latitude (0.5° near the equator), with 44 vertical levels.

Precipitation data are taken from the Global Precipitation Climatology Project (GPCP) version 2.3 data set (Adler *et al.*, 2003). Sea level pressure observations are taken from the Hadley Centre Sea Level Pressure reconstruction version 2 (HadSLP2) data set (Allan and Ansell, 2006) and observational analyses of geopotential height are from ERA-Interim (Dee *et al.*, 2011). Sea surface temperature observations are from the Hadley Centre Sea Ice and Sea Surface Temperature version 2 (HadISST2) data set (Titchner and Rayner, 2014).

3 | PREDICTION SKILL

The largest mean rainfall and the largest inter-annual variability in seasonal rainfall totals occurs in the Tropics (Figure 1). The intense year-to-year variability of boreal winter rainfall is also well connected to extratropical predictions via teleconnections that are thought to be mediated by Rossby waves (Hoskins and Karoly, 1981). Following Scaife *et al.* (2017), we examine rainfall predictions for four tropical regions that show high variability and are connected to the extratropical winter circulation in models and observations: the tropical Indian Ocean (TIO: 45°–100°E, 5°S–10°N), tropical West Pacific (TWP: 110°–140°E, 5°S–25°N), tropical East Pacific (TEP: 200°–90°W, 5°S–10°N) and tropical Atlantic (TA: 60°–0°W, 5°S–5°N) shown by the black boxes in Figure 1. Prediction skill for each of the models and each of the four ocean basin regions is measured

by ensemble mean correlations with GPCP data and illustrated in Figure 2. Raw ensemble mean rainfall predictions are plotted in each case to illustrate any bias and the ensemble mean variability from year to year. It is immediately clear that most models and regions are biased wet, as is typically found in climate models (Mueller and Seneviratne, 2014). For all of these regions, scores calculated using different sized ensembles converge quickly with ensemble sizes of 10–15 members being enough for correlation scores to converge (not shown). Consistent with this, the ensemble mean variance is also comparable to that in the observations, suggesting that a large proportion of observed rainfall variability is predictable.

Figure 2 shows that tropical West Pacific rainfall is well predicted by current seasonal forecast systems, with correlations ranging from 0.68 to 0.90 with seasonal mean GPCP rainfall observational data. However, a clear wet bias of around 30% is again present in predicted rainfall. Interestingly, although it does not have higher skill in this region, the BCC model shows a very small bias compared to other models.

Skilful seasonal predictions of tropical Indian Ocean rainfall are produced by most prediction systems (Figure 2), although results are varied and correlations range from small positive values to almost 0.7. Models are again generally too wet with around 30% too much rainfall in most cases. Interestingly the BCC model again shows only a very small mean bias, but this does not relate to its prediction skill which is in the middle of the range from other systems. Many models correctly predict a dip in the 1997/1998 winter and peaks in the 1998/1999 and 2006/2007 winters.

Predictions of tropical Atlantic rainfall show encouraging skill (Figure 2) but the levels vary between systems, with scores ranging from 0.49 to 0.83. All are highly significant, but the skill is lower here than in the tropical West Pacific in almost all prediction systems. Mean biases are more mixed in the Atlantic than the Indian or Pacific basins and over this region biases are generally smaller, with a range of wet and dry biases across different prediction systems.

The prediction systems show near perfect skill scores for the tropical East Pacific region (Figure 2) due mainly to ENSO as we show below. All systems correctly predict the peaks during El Niño and troughs during La Niña but here again a wet bias is evident in almost all systems, although biases are small in the CMCC and KCM models. The BCC and MIROC systems also show suppressed inter-annual anomalies compared to other models. Nevertheless, for this region the very high correlation scores suggest that almost all inter-annual variability is predictable on seasonal timescales.

We should note that these results are also lower bounds on the predictability of tropical rainfall due to the finite ensemble sizes (see model descriptions), inevitable errors in the individual forecast systems and errors in the observations

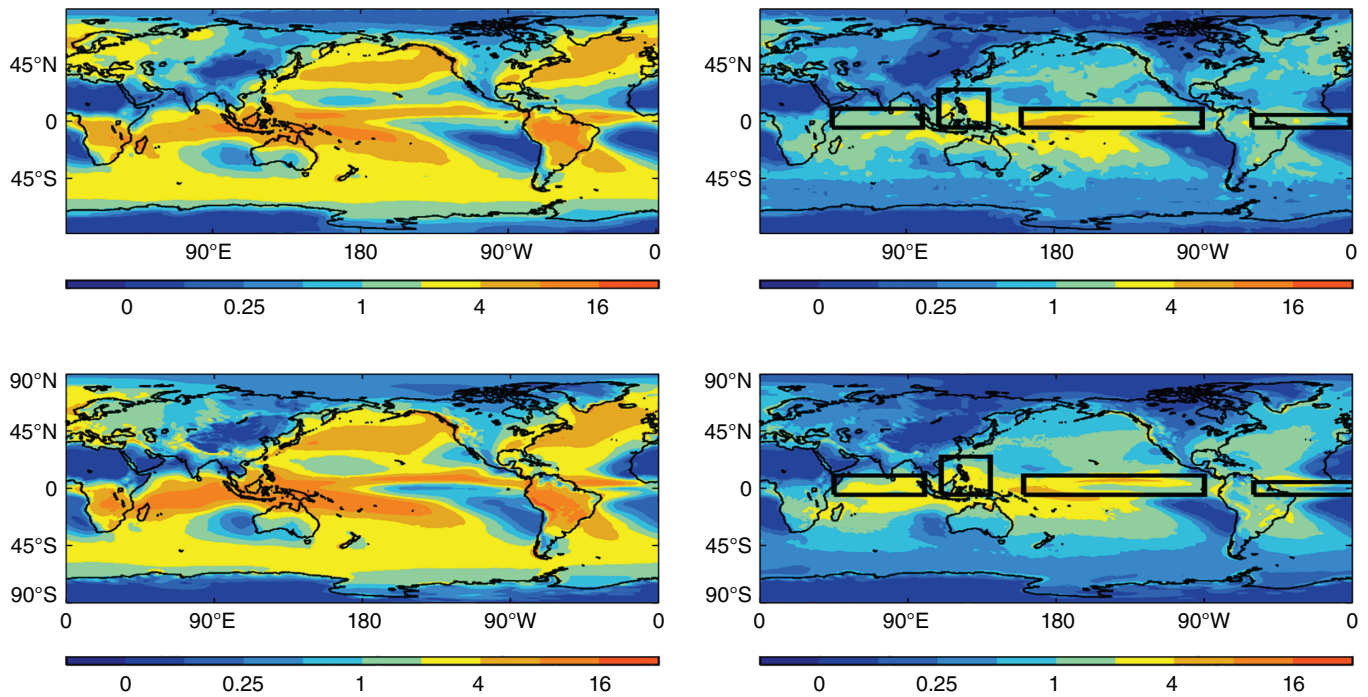


FIGURE 1 Tropical rainfall and its year-to-year variability. Seasonal mean climatological rainfall (top left) and inter-annual variability (top right) of global rainfall from GPCP observations. Tropical rainfall is analysed in the boxed regions for the Indian (45° – 100° E, 5° S– 10° N), West Pacific (110° – 140° E, 5° S– 25° N), East Pacific (200° – 90° W, 5° S– 10° N) and Atlantic (60° – 0° W, 5° S– 5° N) regions (after Scaife *et al.*, 2017). Mean and standard deviation of ensemble member rainfall over the same years (1993–2012) from a single example prediction system (bottom panels, GloSea5). Note the logarithmic contour interval. Units are mm/day

used for initialization and verification. It is common practice to increase ensemble size and remove some of these errors by cancellation by taking multi-model mean forecasts (dashed lines in Figure 2). In our case this results in an ensemble size of over 100 members and this multi-model average shows the best overall scores (Figure 2, inset scores in black). However, the multi-model mean still shows similar skill levels to the best single model in each region. This similar skill, despite the much larger multi-model ensemble size, is consistent with rapid convergence of skill for tropical rainfall (Kumar and Chen, 2015). As in the single model cases, there is a clear ranking of skill across the different regions with TEP > TWP > TA > TIO. We offer an explanation for this ranking below when we consider teleconnections to the El Niño–Southern Oscillation.

4 | MODELLED PREDICTABILITY

It is important to distinguish the predictability of the real climate system from that in prediction systems, as these may not always be the same (Kumar *et al.*, 2014a). Neither is modelled predictability an upper estimate of the real-world predictability as is often assumed. A few studies have tried to estimate seasonal predictability from analysis of observations alone (e.g., Keeley *et al.*, 2009; Feng *et al.*, 2012) but we can estimate the predictability of the real world directly by taking correlations between ensemble mean forecasts and observations. Similarly, we can estimate the predictability of

the model by substituting single ensemble members for the observations and correlating with the mean of the remaining members. Of course, if our prediction systems (and the climate models they contain) were perfect then these two measures would be statistically identical. This is the crucial assumption in so called “perfect model” studies where modelled predictability is used to estimate real-world predictability. However, this is not always the case, and examples have been found where the predictability of the model is either higher or lower than that of the real world (e.g., Eade *et al.*, 2014; Scaife *et al.*, 2014; Seviour *et al.*, 2014; Weisheimer and Palmer, 2014; Kumar *et al.*, 2014a; Dunstone *et al.*, 2016; Kumar and Chen, 2017; Saito *et al.*, 2017).

Figure 3 compares the predictability of the models with their skill in predicting the observations. One value is plotted for each model and each region. Perfect models would lie close to the diagonal line where the model skill in predicting one of its own ensemble members equals its skill of predicting the real world. For the TEP region we can see this is almost the case as predictions are near perfect on this time-scale, although even here, prediction systems are slightly better at predicting themselves than the observations. In the TWP, modelled predictability is again close to prediction skill, with similar high (typically ~ 0.8) correlations when the ensemble mean is compared with single ensemble members or observations alike. For the tropical Atlantic rainfall almost all models show a greater correlation with their own ensemble members than with the observations, suggesting they are

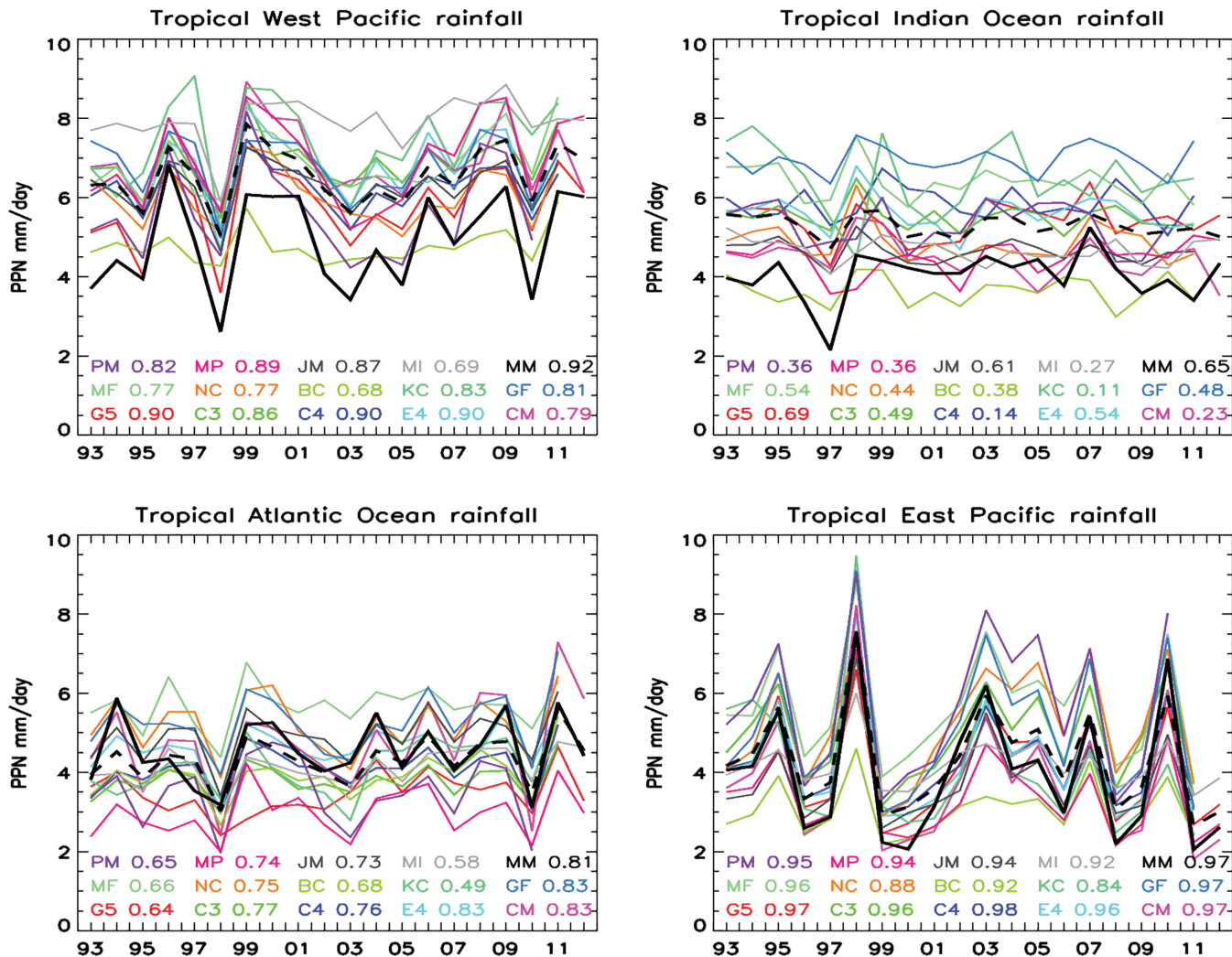


FIGURE 2 Prediction skill of winter rainfall for the tropical West Pacific, Indian, Atlantic and East Pacific Ocean regions. Absolute winter mean rainfall values are plotted (mm/day) from the ensemble mean of each forecast system: BC = BCC, KC = KCM, GF = GFDL, PM = POAMA, MP = MPI, JM = JMA, MI = MIROC, G5 = UKMO, C3 = CANCM3, C4 = CANCM4, E4 = ECMWF, CM = CMCC, MF = METEOF, NC = NCEP. GPCP observational data (solid black) and multi-model mean (dashed black). Correlation scores are inset

overconfident, or equivalently, that they are better at predicting themselves than the real-world rainfall variability. Finally, the Indian Ocean rainfall shows the largest errors: almost all models are overconfident and correlations of the ensemble mean with single model ensemble members are around twice as large as the correlations with observations.

As noted by other studies, this overconfidence can present serious problems with the use of forecasts (Weisheimer and Palmer, 2014). Depending on its cause, overconfidence may also indicate a potential for high skill if systematic errors can be corrected. For example, a systematic error in the spatial structure of a predictable teleconnection could lead to overconfident forecasts. If this teleconnection were improved in future climate models and hence future seasonal forecast systems, then skill could in principle rise. However, we also note that if the overconfidence of rainfall forecasts for the Indian Ocean is due to the absence of *unpredictable* “noise” in models, from weak model representation of the

Madden–Julian Oscillation for example, then there may actually be limited potential for improvement.

5 | INTER-BASIN CONNECTIONS AND THE EFFECTS OF ENSO

Atmospheric variability over the tropical oceans is correlated across different ocean basins (e.g., Camberlin *et al.*, 2004; Kumar *et al.*, 2014b; Molteni *et al.*, 2015; Scaife *et al.*, 2017). These links arise primarily due to changes in atmospheric circulation that can bridge land regions and create remote teleconnections, often due to ENSO (e.g., Giannini *et al.*, 2001; Dong *et al.*, 2006; Toniazzo and Scaife, 2006; Smith *et al.*, 2010). If we are to extract the maximum prediction skill from globally important sources of predictability such as ENSO, it is therefore important to have good teleconnections between rainfall over different tropical ocean basins.

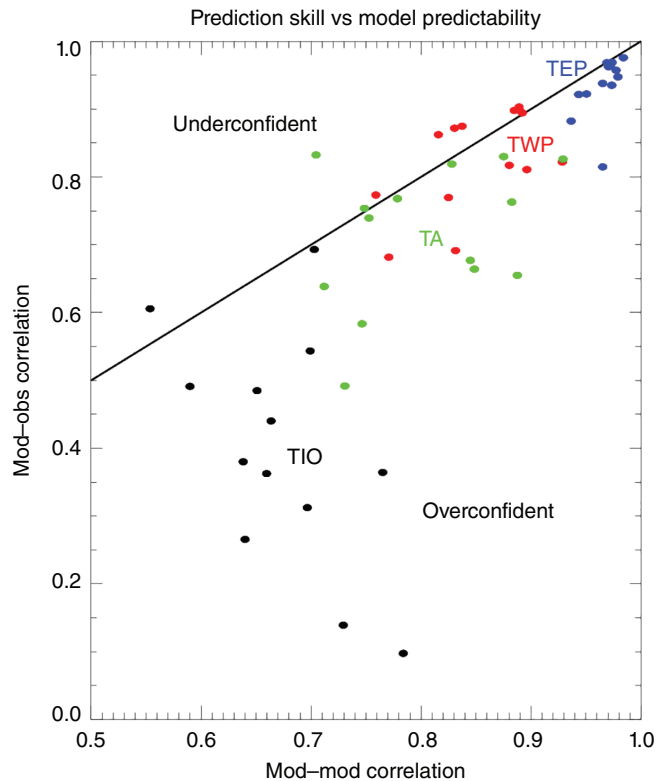


FIGURE 3 Model predictability versus real-world prediction skill. Skill in predicting observations is plotted against modelled predictability for each region and each prediction system. Modelled predictability is calculated as the average correlation between single forecast members and the ensemble mean of the remaining members

The skill of seasonal predictions of tropical rainfall is found to be generally high in our analysis (Figure 2). However, inter-basin connections are more uncertain because, unlike deterministic prediction skill which involves the ensemble *mean*, model inter-basin relationships can only be meaningfully compared to observations using the correlation across basins in individual ensemble *members*, which will therefore contain significant unpredictable internal variability. Some of these statistics can therefore vary substantially across the GPCP observational record due to sampling variability. To try and address this sampling variability we therefore examine inter-basin connections from all the forecast systems by calculating the correlation between rainfall in pairs of tropical regions using single ensemble members (c.f., Johnson *et al.*, 2017). Table 1 shows the strength of these relationships in observations and single model ensemble members. In observations, the strongest relationship is found in the anti-correlation between rainfall in the tropical East and West Pacific; as would be expected given the east–

west seesaw in Pacific rainfall due to ENSO. Strong anti-correlation is also found between the tropical East Pacific and the neighbouring tropical Atlantic. Consistent with these results, a positive correlation occurs between rainfall in the West Pacific and that in the tropical Atlantic. Finally, East Pacific/West Pacific rainfall is positively/negatively correlated with that in the Indian Ocean in this season and there is only a weak relationship between Atlantic and Indian Ocean rainfall variations. Table 1 also shows the corresponding range of values from ensemble members and the number of individual models whose member correlations span the value found in observations. It is immediately clear from the range of correlations found in ensemble members that the observed inter-basin relationships are captured by the multi-model ensemble as a whole. A very broad range of correlations is generated and so it is hard to argue that inter-basin connections are misrepresented in the multi-model ensemble. However, it is possible to show that the correlations found in members from *individual* models (Table 1, third row) do not span the value found in observations. It is interesting to note that despite the very high skill in predicting tropical East Pacific rainfall, its inter-basin connections are least well represented and are often weaker than observed, particularly between the East and West Pacific, but also elsewhere, and so this is an important area where seasonal prediction systems might be improved in future.

Many studies note that seasonal predictions are more skilful during periods when ENSO is active (e.g., Arribas *et al.*, 2011; Kim *et al.*, 2012; Lu *et al.*, 2017) so an obvious question is whether the ENSO influence on the different basins is properly represented in current forecast systems. The top left panel of Figure 4 shows the strength of predicted year-to-year variations in tropical rainfall in each of our four regions, calculated as the standard deviation of the multi-model ensemble mean. In order of magnitude, the largest predictable signals are found in the East Pacific, West Pacific, Atlantic and Indian Ocean, which shows the smallest predictable signal. Interestingly, the same ranking is found in the magnitude of observed inter-annual variability (Figure 4, top right) and also in the skill of our multi-model predictions (Figure 2). Figure 4, bottom panels show the signal from a typical ENSO event, obtained by regressing the Niño3.4 SST index against observed and predicted rainfall and scaling to a 2 K ENSO event. The strength of the ENSO signals is lower than observed but within the observational uncertainty in all basins. Note that the strength of ENSO effects follows exactly the same ranking as the skill and

TABLE 1 Observed and modelled inter-basin rainfall correlations. Observed inter-basin correlations (top row), range of inter-basin correlations from all models and all ensemble members (middle row) and number of models whose individual member correlations span the observed correlation (bottom row)

	TEP-TWP	TEP-TA	TEP-TIO	TWP-TA	TWP-TIO	TA-TIO
Observed	-0.89	-0.62	+0.41	+0.61	-0.30	-0.07
Modelled	-0.96, -0.24	-0.85, 0.16	-0.67, 0.75	-0.09, 0.83	-0.65, 0.64	-0.69, 0.75
No. models spanning obs.	6/14	10/14	9/14	12/14	11/14	11/14

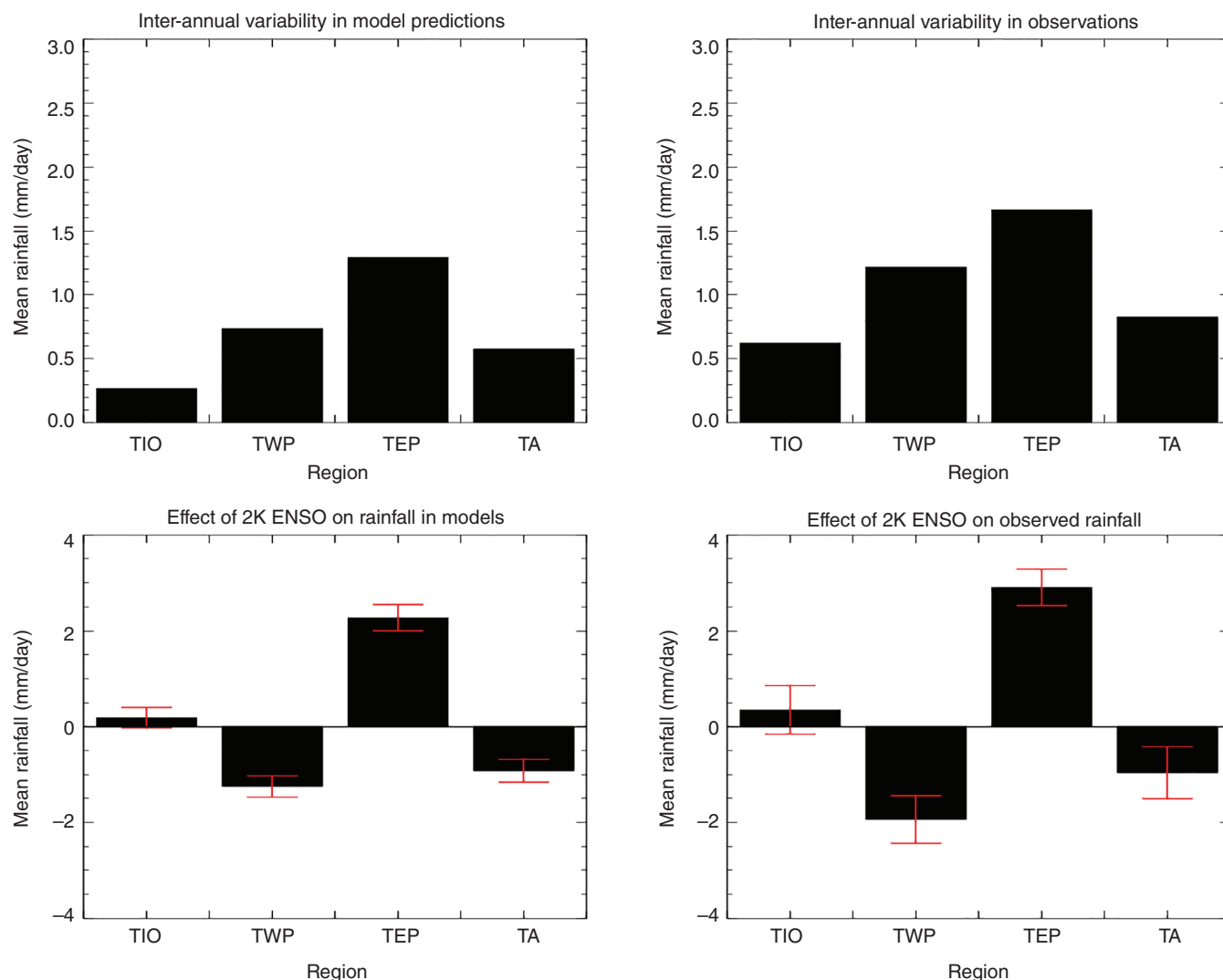


FIGURE 4 Impact of ENSO on tropical rainfall predictions. Mean rainfall in the four tropical regions from the multi model mean (top left) and observations (top right). ENSO anomalies in rainfall in the four regions (bottom panels) are calculated by linear regression of multi model predictions against Niño3.4 and correspond to a 2 K warm anomaly. 95% uncertainty ranges are shown for both model and observations. Units are mm/day

inter-annual variability of different basins. The observed variability, the size of predictable signals and the relative skill of seasonal predictions for different basins can therefore be explained by the relative strength of the ENSO influence on each basin. Indeed, when we removed the ENSO influence from forecasts for each basin using linear regression on Niño3.4, only small and statistically insignificant (but positive) levels of skill remained (not shown).

6 | WHAT GOVERNS PREDICTION SKILL?

So far we have examined anomalies from the climatological mean of forecasts for many years, after linearly correcting away the mean bias in each of the models. However, initialized predictions from different systems drift to a greater or lesser degree (e.g., Hermanson *et al.*, 2017) and if the resulting bias from the real world is large enough, then it could be that this affects the skill of predictions (e.g., Magnusson

et al., 2013; Smith *et al.*, 2013; Vecchi *et al.*, 2014; Kim *et al.*, 2017). We therefore examined the prediction skill for different regions as a function of model bias.

The skill of rainfall predictions from each forecast system for the same four regions was compared with the corresponding mean rainfall bias in each system. For the tropical West Pacific, tropical East Pacific and tropical Indian Ocean, correlations between skill and mean bias across the systems were 0.0, 0.1 and -0.1 , respectively, indicating no simple systematic relationship between mean rainfall bias and the skill of predictions. This is a simple test for a link between mean bias and skill and it could be that mean biases in other variables control both the mean rainfall and prediction skill (c.f., Magnusson *et al.*, 2013; Richter, 2015; Mulholland *et al.*, 2017). Nevertheless, it suggests that if we were to focus exclusively on improving the mean rainfall biases in these regions in future models, the skill of our seasonal climate predictions may not be improved. In the tropical Atlantic there is a weak relationship between rainfall bias and

prediction skill ($r = -0.3$). Although it is not statistically significant, this inverse relationship between bias and prediction skill in different systems is what would be expected if model bias were having a detrimental effect on forecast skill. Alleviating model bias in this region might therefore yield higher prediction skill. This possibility is supported by Ding *et al.* (2015). Using the KCM with a correction to surface heat fluxes to reduce SST biases, they improved the fidelity of their data assimilation runs in boreal summer (JJA) and showed a greater role for ocean dynamics in the variability of the tropical Atlantic (Dippe *et al.*, 2017).

If a small mean bias is not sufficient for high prediction skill, then what is? Given the strong influence of ENSO on observed inter-annual variability, forecast inter-annual variability and the ranking of skill across different basins identified above, we now test whether prediction skill is related to the strength of teleconnections to the East Pacific (ENSO) region. Figure 5 shows the relationship between prediction skill and the strength of inter-basin teleconnections to the East Pacific rainfall for each of the other three basins. Most models underestimate the strength of inter-basin teleconnections and clear relationships are now found with prediction skill, which increases as the strength of the teleconnections to the East Pacific increases. The skill of rainfall predictions in the tropical West Pacific and the Indian Ocean are strongly related to the strength of their relationship with the East Pacific.

At this point, we need to be careful about what we conclude from the relationships in Figure 5. For example, if the TIO variability originates from two components: one being the ENSO signal, and the other being poorly predicted but nearly uncorrelated with ENSO, then the correlation skill of predicted TIO rainfall would necessarily be an increasing function of the variance explained by ENSO, as seen in Figure 5. However, we note that the observed relationship between the TIO or TWP and ENSO is *larger* than the model correlation in almost all cases, even though model data are from the ensemble mean and observed data are single realizations. This is surprising given that we might

expect larger correlations from the ensemble mean data and is consistent with the model under-representing the observed inter-basin correlation, at least over this period. In summary, while it is also important to enhance the predictive skill for non-ENSO-related variability where possible, our analysis suggests that errors in inter-basin connections may limit current prediction skill.

7 | LINKS TO EXTRATROPICAL CLIMATE

Seasonal predictions for the extratropics generally show much less skill than for the Tropics (e.g., Kim *et al.*, 2012) but robust skill has previously been established for the Pacific North American (PNA) pattern via skilful predictions of ENSO (e.g., Derome *et al.*, 2005; Athanasiadis *et al.*, 2014) and more recently for the North Atlantic Oscillation (NAO) via skilful predictions of the Tropics (e.g., Greatbatch *et al.*, 2012; Scaife *et al.*, 2014; 2017). International projects are now focusing on these mechanisms as a route to improved climate predictions for the whole globe (e.g., Merryfield *et al.*, 2017).

We determine the potential for skilful prediction of the main modes of extratropical inter-annual variability using our multi-model tropical rainfall predictions alone. The PNA is defined using the index of Wallace and Gutzler (1981) applied to upper tropospheric (200 hPa) geopotential height and the NAO is defined according to the sea level pressure difference between Iceland and the Azores (see Figures 6 and 7, respectively, and figure captions for detailed definitions). Multiple linear regression was then carried out between rainfall in our four tropical regions and these observed PNA and NAO indices (c.f., Scaife *et al.*, 2017).

Figures 6 and 7, middle panels show the strong relationship between observed winter rainfall variations and associated variability in the PNA (Figure 6) and the NAO (Figure 7). Using observed winter mean rainfall suggests that perfect advance knowledge of rainfall in our four regions would allow highly skilful predictions of both the

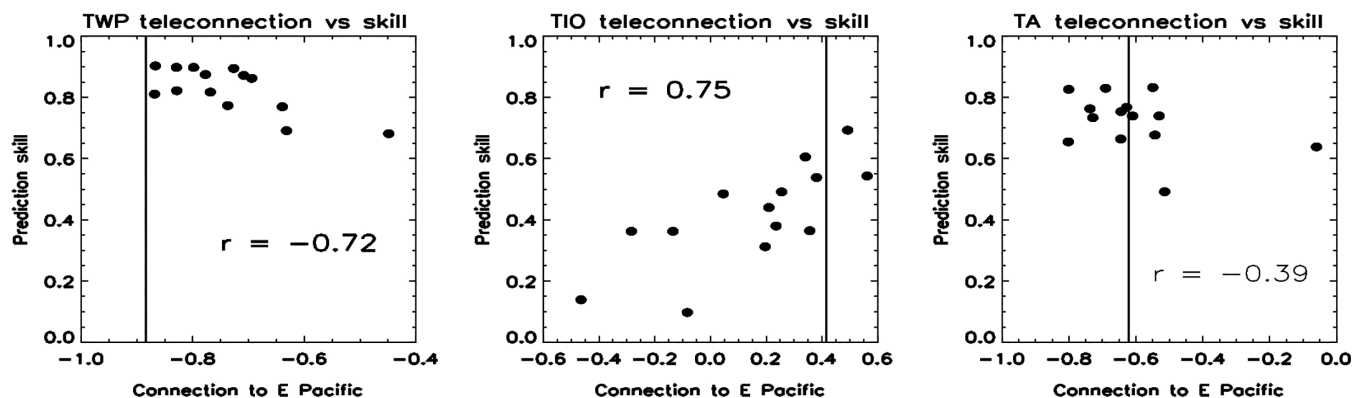


FIGURE 5 Relationship between prediction skill and inter-basin rainfall correlations. Prediction skill for rainfall from each system is plotted against the inter-basin correlation between rainfall in that region and rainfall in the tropical East Pacific (ENSO) region. The vertical lines represent the observed correlation

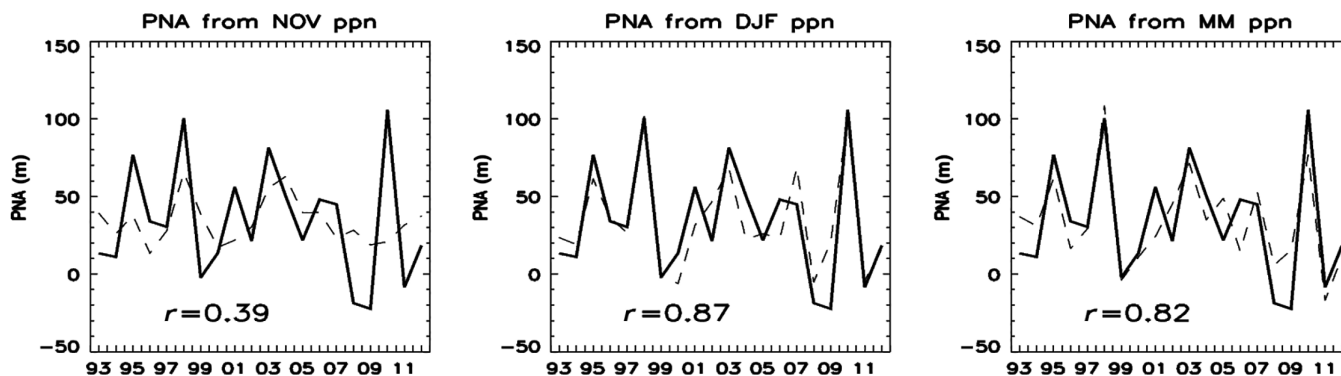


FIGURE 6 Tropical rainfall predictions allow skilful prediction of the Pacific North American pattern. Predictions of the PNA index: $(Z(20\text{ N}, 160\text{ W}) - Z(45\text{ N}, 165\text{ W}) + Z(55\text{ N}, 115\text{ W}) - Z(30\text{ N}, 85\text{ W}))/4$ calculated from the 200 hPa geopotential height (m). Predictions are made using linear regression of the four rainfall indices used in this study and observed rainfall for November (left), observed rainfall for December–February (middle) and multi-model predictions (right)

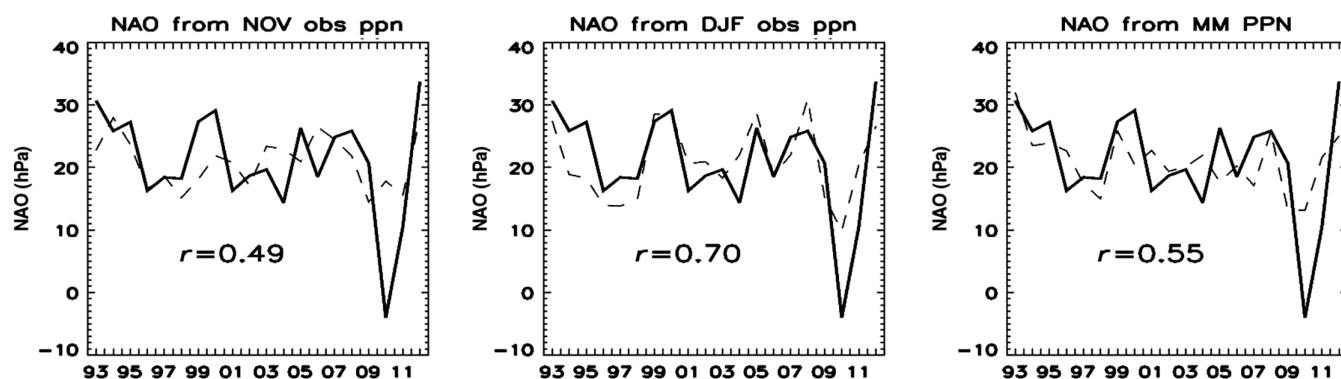


FIGURE 7 Tropical rainfall predictions allow skilful prediction of the North Atlantic Oscillation. Predictions of the NAO index: mean sea level pressure difference (hPa) between Iceland (23 W, 65 N) and the Azores (26 W, 38 N). Predictions are made from linear regression of the four rainfall indices used in this study and observed rainfall for November (left), observed rainfall for December–February (middle) and multi-model predictions (right)

PNA ($r = 0.87$) and the NAO ($r = 0.70$). Of course in practice, the observed winter rainfall is not known in advance but some skill can even be derived from knowledge of November rainfall, with significant, though lower, correlations of 0.39 and 0.49 for the PNA and NAO, respectively. Multi-model predictions of tropical rainfall improve on these empirical forecast scores with correlations of 0.82 (PNA) and 0.55 (NAO), and reach even higher values in some single models, confirming that skilful predictions of tropical rainfall are likely to be crucial for the prediction of major modes of extratropical winter variability.

8 | CONCLUSIONS

We find encouraging levels of tropical winter rainfall prediction skill on seasonal timescales in different forecast systems. High levels of skill are found in tropical rainfall predictions in all basins and a very similar pattern emerges across different forecast systems: the East Pacific is the most predictable region, followed by the West Pacific, then the Atlantic and finally the Indian region. Our multi-model-

mean predictions suggest that the proportion of observed rainfall variance that is predictable in each basin is at least:

$$\text{TEP}(94\%) > \text{TWP}(85\%) > \text{TA}(67\%) > \text{TIO}(42\%).$$

Furthermore, we find an identical ranking in the observed levels of inter-annual variability, in the magnitude of predicted ensemble mean signals and in the influence of ENSO on each of these regions. This striking similarity, and the fact that only small levels of skill remain after ENSO variability is linearly removed from the forecasts, suggests that the skill of tropical rainfall in current seasonal forecast systems is largely driven by ENSO. However, the imperfect correlations between rainfall in the East Pacific and other regions, the imperfect correlation between the inferred NAO and PNA forecasts shown here, and the (small) but positive residual skill in each basin after ENSO is linearly removed all suggest that a single ENSO index is not sufficient to explain all tropical rainfall variability.

Unlike the extratropics, the signal to noise ratio in tropical rainfall forecasts is very large and relatively few ensemble members (<15) are needed to realize almost all of the available prediction skill (Kumar and Chen, 2015). Modelled predictability is generally higher than the skill in predicting

observed variations, suggesting overconfidence, especially over the Indian Ocean, which showed the lowest skill despite remote teleconnections that have been identified for Indian rainfall (e.g., Kucharski *et al.*, 2009; Molteni *et al.*, 2015). This contrasts sharply with the extratropics in the Atlantic for example, where modelled predictability can be lower than the skill of predicting the observations, and models can be *underconfident* (Eade *et al.*, 2014; Scaife *et al.*, 2014; Stockdale *et al.*, 2015; Dunstone *et al.*, 2016; Kumar and Chen, 2017; Saito *et al.*, 2017).

Potential for improvement appears to exist in the Indian Ocean basin, where modelled predictability far exceeds current prediction skill. However, we emphasize that high levels of model predictability does not always indicate potential for improvement and an important caveat here is the lack of realistic MJO activity in models which could itself be unpredictable on seasonal timescales and thereby prevent future improvement in forecast skill. There is also potential for improvement in the Atlantic where model bias may be degrading skill. This is perhaps not surprising given large model biases in the tropical Atlantic, and nearby SST biases that are often large enough to reverse the zonal SST gradient (Richter, 2015). However, no significant relationship was detectable between local biases and prediction skill in the regions we examined. Instead, we point to the very clear relationship between the strength of inter-basin rainfall connections and the skill of model predictions. These connections are often misrepresented in models and focused model development to improve inter-basin rainfall connections would likely yield improved climate predictions.

Overall, our results demonstrate high levels of seasonal predictability in tropical rainfall in all basins and across current seasonal prediction systems. Finally, although there may be some multidecadal variability in skill levels (e.g., Weisheimer *et al.* 2015; Kumar and Chen, 2017), links between tropical rainfall and major modes of extratropical variability such as the PNA and NAO indicate that these highly skilful seasonal predictions of tropical rainfall can drive highly skilful predictions for the extratropics if models can accurately represent the mechanisms of tropical–extratropical interaction.

ACKNOWLEDGEMENTS

This work was supported by the UK-China Research & Innovation Partnership Fund through the Met Office Climate Science for Service Partnership (CSSP) China as part of the Newton Fund and the Joint DECC/Defra Met Office Hadley Centre Climate Programme (GA01101). This paper is also an outcome of the “Interaction/teleconnection between tropics and extratropics” initiative of the World Climate Research Programme’s Working Group on Subseasonal to Seasonal Prediction (WGSIP). We thank the WMO-WCRP for supporting this work and coordinating the CHFP

database through the WGSIP. W.A.M. was supported by the German Ministry of Education and Research (BMBF) under the MiKlip project FLEXFORDEC (Grant No. 01LP1519A). J.B. was supported by the Cluster of Excellence CliSAP (EXC177), Universität Hamburg, funded through the German Science Foundation (DFG). T.C. and R.J.G. acknowledge support from the German Ministry of Education and Science (BMBF) through MiKlip2 subproject ATMOS-MODIN (Grant No. 01LP1517D) and SACUS (Grant No. 03G0837A) and by the European Union 7th Framework Programme (FP7 2007–2013) under Grant agreement 603521 PREFACE project.

ORCID

Adam A. Scaife  <http://orcid.org/0000-0002-5189-7538>

REFERENCES

- Adler, R.F., Huffman, G.J., Chang, A., Ferraro, R., Xie, P., Janowiak, J., Rudolf, B., Schneider, U., Curtis, S., Bolvin, D., Gruber, A., Susskind, J., Arkin, P. and Nelkin, E. (2003) The Version-2 Global Precipitation Climatology Project (GPCP) monthly precipitation analysis (1979–present). *Journal of Hydrometeorology*, 4, 1147–1167. [https://doi.org/10.1175/1525-7541\(2003\)004<1147:TVGPCP>2.0.CO;2](https://doi.org/10.1175/1525-7541(2003)004<1147:TVGPCP>2.0.CO;2).
- Ahn, M.S., Kim, D., Sperber, K.R., Kang, I.-S., Maloney, E., Waliser, D. and Hendon, H. (2017) MJO simulation in CMIP5 climate models: MJO skill metrics and process-oriented diagnosis. *Climate Dynamics*, 49, 4023–4045. <https://doi.org/10.1007/s00382-017-3558-4>.
- Alessandri, A., Borrelli, A., Masina, S., Cherchi, A., Gualdi, S., Navarra, A., Di Pietro, P. and Carril, A.F. (2010) The INGV–CMCC seasonal prediction system: improved ocean initial conditions. *Monthly Weather Review*, 138, 2930–2952. <https://doi.org/10.1175/2010MWR3178.1>.
- Allan, R. and Ansell, T. (2006) A new globally complete monthly historical gridded mean sea level pressure dataset (HadSLP2): 1850–2004. *Journal of Climate*, 19, 5816–5842. <https://doi.org/10.1175/JCLI3937.1>.
- Arakawa, A. (2004) The cumulus parameterization problem: past, present, and future. *Journal of Climate*, 17, 2493–2525.
- Arribas, A., Glover, M., Maidens, A., Peterson, K., Gordon, M., MacLachlan, C., Graham, R., Fereday, D., Camp, J., Scaife, A.A., Xavier, P., McLean, P., Colman, A. and Cusack, S. (2011) The GloSea4 ensemble prediction system for seasonal forecasting. *Monthly Weather Review*, 139, 1891–1910. <https://doi.org/10.1175/2010MWR3615.1>.
- Athanasiadis, P.J., Bellucci, A., Hermanson, L., Scaife, A.A., MacLachlan, C., Arribas, A., Materia, S., Borrelli, A. and Gualdi, S. (2014) The representation of atmospheric blocking and the associated low-frequency variability in two seasonal prediction systems (CMCC, Met-Office). *Journal of Climate*, 27, 9082–9100. <https://doi.org/10.1175/JCLI-D-14-00291.1>.
- Athanasiadis, P.J., Bellucci, A., Scaife, A.A., Hermanson, L., Materia, S., Sanna, A., Borrelli, A., MacLachlan, C. and Gualdi, S. (2017) A multisystem view of wintertime NAO seasonal predictions. *Journal of Climate*, 30, 1461–1475. <https://doi.org/10.1175/JCLI-D-16-0153.1>.
- Baehr, J. and Piontek, R. (2013) Ensemble initialization of the oceanic component of a coupled model through bred vectors at seasonal-to-interannual time scales. *Geoscientific Model Development Discussion*, 6, 5189–5214. <https://doi.org/10.5194/gmdd-6-5189-2013>.
- Baehr, J., Fröhlich, K., Botzet, M., Domeisen, D.I.V., Kornbluh, L., Notz, D., Piontek, R., Pohlmann, H., Tietsche, S. and Müller, W.A. (2015) The prediction of surface temperature in the new seasonal prediction system based on the MPI–ESM coupled climate model. *Climate Dynamics*, 44, 2723–2735. <https://doi.org/10.1007/s00382-014-2399-7>.
- Batté, L. and Déqué, M. (2016) Randomly correcting model errors in the ARPEGE–Climate v6.1 component of CNRM–CM: applications for seasonal forecasts. *Geoscientific Model Development*, 9, 2055–2076. <https://doi.org/10.5194/gmd-9-2055-2016>.
- Camberlin, P., Chauvin, F., Douville, H. and Zhao, Y. (2004) Simulated ENSO–tropical rainfall teleconnections in present-day and under enhanced

- greenhouse gases conditions. *Climate Dynamics*, 23, 641–657. <https://doi.org/10.1007/s00382-004-0460-7>.
- Chang, Y.-S., Zhang, S., Rosati, A., Delworth, T.L. and Stern, W.F. (2013) An assessment of oceanic variability for 1960–2010 from the GFDL ensemble coupled data assimilation. *Climate Dynamics*, 40, 775–803. <https://doi.org/10.1007/s00382-012-1412-2>.
- Cheng, Y.J., Tang, Y.M., Zhou, X.B., et al. (2010) Further analysis of singular vector and ENSO predictability in the Lamont model—part I: singular vector and the control factors. *Climate Dynamics*, 35, 807–826.
- Dee, D.P., Uppala, S.M., Simmons, A.J., Berrisford, P., Poli, P., Kobayashi, S., Andrae, U., Balmaseda, M.A., Balsamo, G., Bauer, P., Bechtold, P., Beljaars, A.C.M., van de Berg, L., Bidlot, J., Bormann, N., Delsol, C., Dragani, R., Fuentes, M., Geer, A.J., Haimberger, L., Healy, S.B., Hersbach, H., Hólm, E.V., Isaksen, I., Kållberg, P., Köhler, M., Matricardi, M., McNally, A.P., Monge-Sanz, B.M., Morcrette, J.-J., Park, B.-K., Peubey, C., de Rosnay, P., Tavolato, C., Thépaut, J.-N. and Vitart, F. (2011) The ERA-Interim reanalysis: configuration and performance of the data assimilation system. *Quarterly Journal of the Royal Meteorological Society*, 137, 553–597.
- Delworth, T.L., Broccoli, A.J., Rosati, A., Stouffer, R.J., Balaji, V., Beesley, J.A., Cooke, W.F., Dixon, K.W., Dunne, J., Dunne, K.A., Durachtae, J.W., Findella, K.L., Ginoux, P., Gnanadesikan, A., Gordona, C.T., Griffies, S.M., Gudgel, R., Harrison, M.J., Held, I.M., Hemler, R.S., Horowitz, L.W., Klein, S.A., Knutson, T.R., Kushner, P.J., Langenhorst, A.R., Lee, H.-C., Lina, S.-J., Lu, J., Malyshev, S.L., Milly, P.C.D., Ramaswamy, V., Russell, J., Schwarzkopf, M.D., Shevliakova, E., Sirutis, J.J., Spelman, M.J., Stern, W.F., Winton, M., Wittenberg, A.T., Wyman, B., Zeng, F. and Zhang, R. (2006) GFDL's CM2 global coupled climate models. Part I: formulation and simulation characteristics. *Journal of Climate*, 19, 643–674.
- Delworth, T.L., Rosati, A., Anderson, W., Adcroft, A.J., Balaji, V., Benson, R., Dixon, K., Griffies, S.M., Lee, H.-C., Pacanowski, R.C., Vecchi, G.A., Wittenberg, A.T., Zeng, F. and Zhang, R. (2012) Simulated climate and climate change in the GFDL CM2.5 high-resolution coupled climate model. *Journal of Climate*, 25, 2755–2781.
- Dequé, M. (2001) Seasonal predictability of tropical rainfall: probabilistic formulation and validation. *Tellus A*, 53, 500–512.
- Derome, J., Lin, H. and Brunet, G. (2005) Seasonal forecasting with a simple general circulation model: predictive skill in the AO and PNA. *Journal of Climate*, 18, 597–609.
- Ding, H., Greatbatch, R.J., Latif, M., Park, W. and Gerdes, R. (2013) Hindcast of the 1976/77 and 1998/99 climate shifts in the Pacific. *Journal of Climate*, 26, 7650–7661. <https://doi.org/10.1175/JCLI-D-12-00626.1>.
- Ding, H., Greatbatch, R.J., Latif, M. and Park, W. (2015) The impact of sea surface temperature bias on equatorial Atlantic interannual variability in partially coupled model experiments. *Geophysical Research Letters*, 42, 5540–5546. <https://doi.org/10.1002/2015GL064799>.
- Dippe, T., Greatbatch, R.J. and Ding, H. (2017) On the relationship between Atlantic Niño variability and ocean dynamics. *Climate Dynamics*, 51, 597–612. <https://doi.org/10.1007/s00382-017-3943-z>.
- Dong, B., Sutton, R.T. and Scaife, A.A. (2006) Multidecadal modulation of El Niño–Southern Oscillation (ENSO) variance by Atlantic Ocean sea surface temperatures. *Geophysical Research Letters*, 33, L08705.
- Dunstone, N., Smith, D., Scaife, A.A., Hermanson, L., Eade, R., Robinson, N., Andrews, M. and Knight, J. (2016) Skilful predictions of the winter North Atlantic Oscillation one year ahead. *Nature Geoscience*, 9, 809–814. <https://doi.org/10.1038/ngeo2824>.
- Dutra, E., Pozzi, W., Wetterhall, F., di Giuseppe, F., Magnusson, L., Naumann, G., Barbosa, P., Vogt, J. and Pappenberger, F. (2014) Global meteorological drought—part 2: seasonal forecasts. *Hydrology and Earth System Sciences*, 18, 2669–2678.
- Eade, R., Smith, D., Scaife, A., Wallace, E., Dunstone, N., Hermanson, L. and Robinson, N. (2014) Do seasonal-to-decadal climate predictions underestimate the predictability of the real world? *Geophysical Research Letters*, 41(15), 5620–5628. <https://doi.org/10.1002/2014GL061146>.
- Feng, X., DelSole, T. and Houser, P. (2012) A method for estimating potential seasonal predictability: analysis of covariance. *Journal of Climate*, 25, 5292–5308. <https://doi.org/10.1175/JCLI-D-11-00342.1>.
- Giannini, A., Chiang, J.C., Cane, M.A., Kushnir, Y. and Seager, R. (2001) The ENSO teleconnection to the tropical Atlantic Ocean: contributions of the remote and local SSTs to rainfall variability in the tropical Americas. *Journal of Climate*, 14, 4530–4544.
- Giorgetta, M.A., Jungclaus, J., Reick, C.H., Legutke, S., Bader, J., Böttinger, M., Brovkin, V., Crueger, T., Esch, M., Fieg, K., Glushak, K., Gayler, V., Haak, H., Hollweg, H.-D., Ilyina, T., Kinne, S., Kornbluh, L., Matei, D., Mauritson, T., Mikolajewicz, U., Mueller, W., Notz, D., Pithan, F., Raddatz, T., Rast, S., Redler, R., Roeckner, E., Schmidt, H., Schnur, R., Segsneider, J., Six, K.D., Stockhause, M., Timmreck, C., Wegner, J., Widmann, H., Wieners, K.-H., Claussen, M., Marotzke, J. and Stevens, B. (2013) Climate and carbon cycle changes from 1850 to 2100 in MPI-ESM simulations for the Coupled Model Intercomparison Project phase 5. *Journal of Advances in Modeling Earth Systems*, 5, 572–597. <https://doi.org/10.1002/jame.20038>.
- Greatbatch, R.J., Gollan, G., Jung, T. and Kunz, T. (2012) Factors influencing Northern Hemisphere winter mean atmospheric circulation anomalies during the period 1960/61 to 2001/02. *Quarterly Journal of the Royal Meteorological Society*, 138, 1970–1982. <https://doi.org/10.1002/qj.1947>.
- Griffies, S.M., Gnanadesikan, A., Dixon, K.W., Dunne, J.P., Gerdes, R., Harrison, M.J., Rosati, A., Russell, J.L., Samuels, B.L., Spelman, M.J., Winton, M. and Zhang, R. (2005) Formulation of an ocean model for global climate simulations. *Ocean Science*, 1, 45–79.
- Hermanson, L., Gnanadesikan, A., Dixon, K.W., Dunne, J.P., Gerdes, R., Harrison, M.J., Rosati, A., Russell, J.L., Samuels, B.L., Spelman, M.J., Winton, M. and Zhang, R. (2017) Different types of drifts in two seasonal forecast systems and dependence on ENSO. *Climate Dynamics*, 51, 1411–1426. <https://doi.org/10.1007/s00382-017-3962-9>.
- Hoskins, B.J. and Karoly, D.J. (1981) The steady linear response of a spherical atmosphere to thermal and orographic forcing. *Journal of the Atmospheric Sciences*, 38, 1179–1196.
- Hudson, D., Alves, O., Hendon, H.H. and Wang, G. (2011) The impact of atmospheric initialisation on seasonal prediction of tropical Pacific SST. *Climate Dynamics*, 36, 1155–1171.
- Hudson, D., Marshall, A.G., Yin, Y., Alves, O. and Hendon, H.H. (2013) Improving intraseasonal prediction with a new ensemble generation strategy. *Monthly Weather Review*, 141, 4429–4449. <https://doi.org/10.1175/MWR-D-13-00059.1>.
- Imada, Y., Tatebe, H., Ishii, M., Chikamoto, Y., Mori, M., Arai, M., Watanabe, M. and Kimoto, M. (2015) Predictability of two types of El Niño assessed using an extended seasonal prediction system by MIROC. *Monthly Weather Review*, 143, 4597–2617.
- Johnson, S.J., Turner, A., Woolnough, S., Martin, G. and MacLachlan, C. (2017) An assessment of Indian monsoon seasonal forecasts and mechanisms underlying monsoon interannual variability in the Met Office GloSea5-GC2 system. *Climate Dynamics*, 48, 1447–1465.
- Jungclaus, J., Fischer, N., Haak, H., Lohmann, K., Marotzke, J., Matei, D., Mikolajewicz, U., Notz, D. and von Storch, J. (2013) Characteristics of the ocean simulations in MPIOM, the ocean component of the MPI-Earth System Model. *Journal of Advances in Modeling Earth Systems*, 5, 422–446. <https://doi.org/10.1002/jame.20023>.
- Kang, D., Lee, M.I., Im, J., Kim, D., Kim, H.-M., Kang, H.-S., Schubert, S.D., Arribas, A. and MacLachlan, C. (2014) Prediction of the Arctic Oscillation in boreal winter by dynamical seasonal forecasting systems. *Geophysical Research Letters*, 41, 3577–3585. <https://doi.org/10.1002/2014GL060011>.
- Keeley, S.P.E., Sutton, R.T. and Shaffrey, L.C. (2009) Does the North Atlantic Oscillation show unusual persistence on intraseasonal timescales? *Geophysical Research Letters*, 36, L22706. <https://doi.org/10.1029/2009GL040367>.
- Kim, H.M., Webster, P.J. and Curry, J.A. (2012) Seasonal prediction skill of ECMWF System 4 and NCEP CFSv2 retrospective forecast for the Northern Hemisphere winter. *Climate Dynamics*, 39, 2957–2973.
- Kim, S.T., Jeong, H.-I. and Jin, F.F. (2017) Mean bias in seasonal forecast model and ENSO prediction error. *Scientific Reports*, 7, 6029. <https://doi.org/10.1038/s41598-017-05221-3>.
- Kirtman, B.P., Min, D., Infanti, J.M., Kinter, J.L., III, Paolino, D.A., Zhang, Q., van den Dool, H., Saha, S., Mendez, M.P., Becker, E., Peng, P., Tripp, P., Huang, J., DeWitt, D.G., Tippett, M.K., Barnston, A.G., Li, S., Rosati, A., Schubert, S.D., Rienecker, M., Suarez, M., Li, Z.E., Marshak, J., and Lim, Y.-K., Tribbia, J., Pegion, K., Merryfield, W.J., Denis, B. and Wood, E.F. (2014) The North American multimodel ensemble: phase-1 seasonal-to-interannual prediction; phase-2 toward developing intraseasonal prediction. *Bulletin of the American Meteorological Society*, 95, 585–601.
- Kobayashi, S., Ota, Y., Harada, Y., Ebata, A., Moriya, M., Onoda, H., Onogi, K., Kamahori, H., Kobayashi, C., Endo, H., Miyaoka, K. and Takahashi, K.

- (2015) The JRA-55 reanalysis: general specifications and basic characteristics. *Journal of Meteorological Society of Japan*, 93, 5–48. <https://doi.org/10.2151/jmsj.2015-001>.
- Kucharski, F., Scaife, A.A., Yoo, J.H., Folland, C.K., Kinter, J., Knight, J., Fereday, D., Fischer, A.M., Jin, E.K., Kröger, J., Lau, N.C., Nakaegawa, T., Nath, M.J., Pegion, P., Rozanov, E., Schubert, S., Sporyshev, P.V., Syktus, J., Voldoire, A., Yoon, J.H., Zeng, N. and Zhou, T. (2009) The CLIVAR C20C project: skill of simulating Indian monsoon rainfall on interannual to decadal timescales. Does GHG forcing play a role? *Climate Dynamics*, 33, 615–627. <https://doi.org/10.1007/s00382-008-0462-y>.
- Kumar, A. and Chen, M. (2015) Inherent predictability, requirements on ensemble size, and complementarity. *Monthly Weather Review*, 143, 3192–3203.
- Kumar, A. and Chen, M. (2017) Causes of skill in seasonal predictions of Arctic Oscillation. *Climate Dynamics*, 51, 2397–2411. <https://doi.org/10.1007/s00382-017-4019-9>.
- Kumar, A., Chen, M. and Wang, W. (2013) Understanding prediction skill of seasonal mean precipitation over the Tropics. *Journal of Climate*, 26, 5674–5681.
- Kumar, A., Peng, P. and Chen, M. (2014a) Is there a relationship between potential and actual skill? *Monthly Weather Review*, 142, 2220–2227.
- Kumar, A., Jha, B. and Wang, H. (2014b) Attribution of SST variability in global oceans and the role of ENSO. *Climate Dynamics*, 43, 209–220.
- Li, S. and Robertson, A.W. (2015) Evaluation of submonthly precipitation forecast skill from global ensemble prediction systems. *Monthly Weather Review*, 143, 2871–2889.
- Li, Y., Li, J., Jin, F.F. and Zhao, S. (2015) Interhemispheric propagation of stationary Rossby waves in a horizontally nonuniform background flow. *Journal of the Atmospheric Sciences*, 72, 3233–3256.
- Liu, X., Wu, T., Yang, S., Jie, W., Nie, S., Li, Q., Cheng, Y. and Liang, X. (2015) Performance of the seasonal forecasting of the Asian summer monsoon by BCC_CSM1.1(m). *Advances in Atmospheric Sciences*, 32, 1156–1172.
- Lu, B., Scaife, A.A., Dunstone, N., Smith, D., Ren, H.-L., Liu, Y. and Eade, R. (2017) Skillful seasonal predictions of winter precipitation over southern China. *Environmental Research Letters*, 12, 074021.
- MacLachlan, C., Arribas, A., Peterson, K.A., Maidens, A., Fereday, D., Scaife, A.A., Gordon, M., Vellinga, M., Williams, A., Comer, R.E., Camp, J., Xavier, P. and Madec, G. (2015) Global seasonal forecast system version 5 (GloSea5): a high-resolution seasonal forecast system. *Quarterly Journal of the Royal Meteorological Society*, 141, 1072–1084. <https://doi.org/10.1002/qj.2396>.
- Madec, G., and the NEMO Team (2008) NEMO ocean engine. Note du Pôle de modélisation, Institut Pierre-Simon Laplace (IPSL), France, 27, 1288–1619.
- Madec, G., and the NEMO Team (1998) NEMO ocean engine. Note du Pôle de modélisation, Institut Pierre-Simon Laplace (IPSL), France, 27, 1288–1619.
- Magnusson, L., Alonso-Balmaseda, M. and Molteni, F. (2013) On the dependence of ENSO simulation on the coupled model mean state. *Climate Dynamics*, 41, 1509–1525. <https://doi.org/10.1007/s00382-012-1574-y>.
- Manabe, S. and Holloway, J. (1975) The seasonal variation of the hydrological cycle as simulated by a global model of the atmosphere. *Journal of Geophysical Research*, 80, 1617–1649. <https://doi.org/10.1029/JC080i012p01617>.
- Materia, S., Borrelli, A., Bellucci, A., Alessandri, A., Di Pietro, P., Athanasiadis, P., Navarra, A. and Gualdi, S. (2014) Impact of atmosphere and land surface initial conditions on seasonal forecasts of global surface temperature. *Journal of Climate*, 27, 9253–9271. <https://doi.org/10.1175/JCLI-D-14-00163.1>.
- Merryfield, W.J., Lee, W.-S., Boer, G.J., Kharin, V.V., Scinocca, J.F., Flato, G. M., Ajayamohan, R.S., Fyfe, J.C., Tang, Y. and Polavarapu, S. (2013) The Canadian seasonal to interannual prediction system. Part I: models and initialization. *Monthly Weather Review*, 141, 2910–2945. <https://doi.org/10.1175/MWR-D-12-00216.1>.
- Merryfield, W.J., Doblas-Reyes, F.J., Ferranti, L., Jeong, J.-H., Orsolini, Y.J., Saurral, R.I., Scaife, A.A., Tolstykh, M.A. and Rixen, M. (2017) Advancing climate forecasting. *Eos*, 98, 17–21. <https://doi.org/10.1029/2017EO086891>.
- Molteni, F., Stockdale, T., Balmaseda, M., Buizza, R., Ferranti, L., Magnusson, L., Mogensen, K., Palmer, T.N. and Vitart, F. (2011) *The new ECMWF seasonal forecast system (system 4)*. Reading: ECMWF. ECMWF technical memorandum number: 656.
- Molteni, F., Stockdale, T.N. and Vitart, F. (2015) Understanding and modelling extra-tropical teleconnections with the Indo-Pacific region during the northern winter. *Climate Dynamics*, 45, 3119–3140. <https://doi.org/10.1007/s00382-015-2528-y>.
- Mueller, B. and Seneviratne, S.I. (2014) Systematic land climate and evapotranspiration biases in CMIP5 simulations. *Geophysical Research Letters*, 41, 128–134. <https://doi.org/10.1002/2013GL058055>.
- Mulholland, D.P., Haines, K., Sparrow, S.N. and Walton, D. (2017) Climate model forecast biases assessed with a perturbed physics ensemble. *Climate Dynamics*, 49, 1729–1746. <https://doi.org/10.1007/s00382-016-3407-x>.
- Newman, M. and Sardeshmukh, P.D. (2017) Are we near the predictability limit of tropical Indo-Pacific sea surface temperatures? *Geophysical Research Letters*, 44, 8520–8529. <https://doi.org/10.1002/2017GL074088>.
- Park, W., Keenlyside, N., Latif, M. and Ströh, A. (2009) Tropical Pacific climate and its response to global warming in the Kiel climate model. *Journal of Climate*, 22, 71–92. <https://doi.org/10.1175/2008JCLI2261.1>.
- Reynolds, R.W., Rayner, N.A., Smith, T.M., Stokes, D.C. and Wang, W. (2002) An improved in situ and satellite SST analysis for climate. *Journal of Climate*, 15, 1609–1625.
- Richter, I. (2015) Climate model biases in the eastern tropical oceans: causes, impacts and ways forward. *WIREs Climate Change*, 6, 345–358. <https://doi.org/10.1002/wcc.338>.
- Riddle, E.E., Butler, A.H., Furtado, J.C., Cohen, J.L. and Kumar, A. (2013) CFSv2 ensemble prediction of the wintertime Arctic Oscillation. *Climate Dynamics*, 41, 1099–1116.
- Roeckner, E., Bäuml, G., Bonaventura, L., Brokopf, R., Esch, M., Giorgetta, M., Hagemann, S., Kirchner, I., Kornbluh, L., Manzini, E., Rhodin, A., Schlese, U., Schulzweida, U. and Tompkins, A. (2003) The atmospheric general circulation model ECHAM5: part 1: model description. *MPI Report*, 249, 1–140. <https://doi.org/10.1029/2010JD014036>.
- Saha, S., Moorthi, S., Pan, H.L., Wu, X., Wang, J., Nadiga, S., Tripp, P., Kistler, R., Woollen, J., Behringer, D., Liu, H., Stokes, D., Grumbine, R., Gayno, G., Wang, J., Hou, Y.T., Chuang, H.Y., Juang, H.M.H., Sela, J., Iredell, M., Treadon, R., Kleist, D., van Delst, P., Keyser, D., Derber, J., Ek, M., Meng, J., Wei, H., Yang, R., Lord, S., van den Dool, H., Kumar, A., Wang, W., Long, C., Chelliah, M., Xue, Y., Huang, B., Schemm, J.K., Ebisuzaki, W., Lin, R., Xie, P., Chen, M., Zhou, S., Higgins, W., Zou, C.Z., Liu, Q., Chen, Y., Han, Y., Cucurull, L., Reynolds, R.W., Rutledge, G. and Goldberg, M. (2010) The NCEP climate forecast system reanalysis. *Bulletin of the American Meteorological Society*, 91, 1015–1057. <https://doi.org/10.1175/2010BAMS3001.1>.
- Saha, S., Moorthi, S., Wu, X., Wang, J., Nadiga, S., Tripp, P., Behringer, D., Hou, Y.-T., Chuang, H.-Y., Iredell, M., Ek, M., Meng, J., Yang, R., Mendez, M.P., van den Dool, H., Zhang, Q., Wang, W., Chen, M. and Becker, E. (2014) The NCEP climate forecast system version 2. *Journal of Climate*, 27, 2185–2208. <https://doi.org/10.1175/JCLI-D-12-00823.1>.
- Saito, N., Maeda, S., Nakaegawa, T., Takaya, Y., Imada, Y. and Matsukawa, C. (2017) Seasonal predictability of the North Atlantic Oscillation and zonal mean fields associated with stratospheric influence in JMA/MRI-CPS2. *SOLA*, 13, 209–213. <https://doi.org/10.2151/sola.2017-038>.
- Scaife, A.A., Arribas, A., Blockley, E., Brookshaw, A., Clark, R.T., Dunstone, N., Eade, R., Fereday, D., Folland, C.K., Gordon, M., Hermanson, L., Knight, J.R., Lea, D.J., MacLachlan, C., Maidens, A., Martin, M., Peterson, A.K., Smith, D., Vellinga, M., Wallace, E., Waters, J. and Williams, A. (2014) Skillful long range prediction of European and North American winters. *Geophysical Research Letters*, 41, 2514–2519. <https://doi.org/10.1002/2014GL059637>.
- Scaife, A.A., Comer, R.E., Dunstone, N.J., Knight, J.R., Smith, D.M., MacLachlan, C., Martin, N., Peterson, K.A., Rowlands, D., Carroll, E.B., Belcher, S. and Slingo, J. (2017) Tropical rainfall, Rossby waves and regional winter climate predictions. *Quarterly Journal of the Royal Meteorological Society*, 143, 1–11. <https://doi.org/10.1002/qj.2910>.
- Schiller, A., Godfrey, J., McIntosh, P. and Meyers, G. (1997) *A global ocean general circulation model climate variability studies*. Canberra: CSIRO. Marine research report number: 227.
- Schiller, A., Godfrey, J., McIntosh, P., Meyers, G., Smith, N., Alves, O., Wang, O. and Fiedler, R. (2002) *A new version of the Australian community ocean model for seasonal climate prediction*. Canberra: CSIRO. Marine research report number: 240.
- Scinocca, J.F., McFarlane, N., Lazare, M. and Li, J. (2008) The CCCma third generation AGCM and its extension into the middle atmosphere. *Atmospheric Chemistry and Physics*, 8, 7055–7074.

- Seviour, W.J., Hardiman, S.C., Gray, L.J., Butchart, N., MacLachlan, C. and Scaife, A.A. (2014) Skillful seasonal prediction of the southern annular mode and Antarctic ozone. *Journal of Climate*, 27, 7462–7474. <https://doi.org/10.1175/JCLI-D-14-00264.1>.
- Simmons, A.J., Wallace, J.M. and Branstator, G.W. (1983) Barotropic wave-propagation and instability, and atmospheric teleconnection patterns. *Journal of the Atmospheric Sciences*, 40, 1363–1392.
- Smith, D.M., Eade, R., Dunstone, N.J., Fereday, D., Murphy, J.M., Pohlmann, H. and Scaife, A.A. (2010) Improved climate model predictions of multi-year North Atlantic hurricane frequency. *Nature Geoscience*, 3, 846–849. <https://doi.org/10.1038/ngeo1004>.
- Smith, D.M., Eade, R. and Pohlmann, H. (2013) A comparison of full-field and anomaly initialization for seasonal to decadal climate prediction. *Climate Dynamics*, 41, 3325–3338. <https://doi.org/10.1007/s00382-013-1683-2>.
- Smith, D.M., Booth, B.B.B., Dunstone, N.J., Eade, R., Hermanson, L., Jones, G. S., Scaife, A.A., Sheen, K.L. and Thompson, V. (2016) Role of volcanic and anthropogenic aerosols in the recent global surface warming slowdown. *Nature Climate Change*, 6, 936–940. <https://doi.org/10.1038/NCLIMATE3058>.
- Stevens, B., Giorgetta, M., Esch, M., Mauritsen, T., Crueger, T., Rast, S., Salzmann, M., Schmidt, H., Bader, J., Block, K., Brokopf, R., Fast, I., Kinne, S., Kornbluh, L., Lohmann, U., Pincus, R., Reichler, T. and Roeckner, E. (2013) The atmospheric component of the MPI-M earth system model: ECHAM6. *Journal of Advances in Modeling Earth Systems*, 5, 146–172.
- Stern, H. and Davidson, N.E. (2015) Trends in the skill of weather prediction at lead times of 1–14 days. *Quarterly Journal of the Royal Meteorological Society*, 141, 2726–2736. <https://doi.org/10.1002/qj.2559>.
- Stockdale, T.N., Anderson, D.L.T., Alves, J.O.S. and Balmaseda, M. (1998) Global seasonal rainfall forecasts using a coupled ocean–atmosphere model. *Nature*, 392, 370–373.
- Stockdale, T.N., Molteni, F. and Ferranti, L. (2015) Atmospheric initial conditions and the predictability of the Arctic Oscillation. *Geophysical Research Letters*, 42, 1173–1179. <https://doi.org/10.1002/2014GL062681>.
- Takaya, Y., Hirahara, S., Yasuda, T., Matsueda, S., Toyoda, T., Fujii, Y., Sugimoto, H., Matsukawa, C., Ishikawa, I., Mori, H., Nagasawa, R., Kubo, Y., Adachi, N., Yamanaka, G., Kuragano, T., Shimpo, A., Maeda, S. and Ose, T. (2017) Japan Meteorological Agency/Meteorological Research Institute-Coupled Prediction System version 2 (JMA/MRI-CPS2): atmosphere–land–ocean–sea ice coupled prediction system. *Climate Dynamics*, 50, 751–765. <https://doi.org/10.1007/s00382-017-3638-5>.
- Tatebe, H., Ishii, M., Mochizuki, T., Chikamoto, Y., Sakamoto, T.T., Komuro, Y., Mori, M., Yasunaka, S., Watanabe, M., Ogochi, K., Suzuki, T., Nishimura, T. and Kimoto, M. (2012) The initialization of the MIROC climate models with hydrographic data assimilation for decadal prediction. *Journal of Meteorological Society of Japan*, 90A, 275–294.
- Thoma, M., Greatbatch, R.J., Kadow, C. and Gerdes, R. (2015) Decadal hindcasts initialized using observed surface wind stress: evaluation and prediction out to 2024. *Geophysical Research Letters*, 42, 6454–6461. <https://doi.org/10.1002/2015GL064833>.
- Titchner, H.A. and Rayner, N.A. (2014) The Met Office Hadley Centre sea ice and sea surface temperature data set, version 2: 1. Sea ice concentrations. *Journal of Geophysical Research: Atmospheres*, 119, 2864–2889. <https://doi.org/10.1002/2013JD020316>.
- Toniazzo, T. and Scaife, A.A. (2006) The influence of ENSO on winter North Atlantic climate. *Geophysical Research Letters*, 33, L24704. <https://doi.org/10.1029/2006GL027881>.
- Toyoda, T., Fujii, Y., Yasuda, T., Usui, N., Iwao, T., Kuragano, T. and Kamachi, M. (2013) Improved analysis of the seasonal interannual fields by a global ocean data assimilation system. *Theoretical and Applied Mechanics Japan*, 61, 31–48.
- Trenberth, K.E., Fasullo, J.T., Branstator, G. and Phillips, A.S. (2014) Seasonal aspects of the recent pause in surface warming. *Nature Climate Change*, 4, 911–916.
- Valcke, S. (2013) The OASIS3 coupler: a European climate modelling community software. *Geoscientific Model Development Discussions*, 5(3), 2139–2178. <https://doi.org/10.5194/gmdd-5-2139-2012>.
- Vecchi, G.A., Delworth, T., Gudgel, R., Kapnick, S., Rosati, A., Wittenberg, A. T., Zeng, F., Anderson, W., Balaji, V., Dixon, K., Jia, L., Kim, H.-S., Krishnamurthy, L., Msadek, R., Stern, W.F., Underwood, S.D., Villarini, G., Yang, X. and Zhang, S. (2014) On the seasonal forecasting of regional tropical cyclone activity. *Journal of Climate*, 27, 7994–8016.
- Voldoire, A., Sanchez-Gomez, E., Salas y Méliá, D., Decharme, B., Cassou, C., Sénési, S., Valcke, S., Beau, I., Alias, A., Chevallier, M., Déqué, M., Deshayes, J., Douville, H., Fernandez, E., Madec, G., Maisonnave, E., Moine, M.-P., Planton, S., Saint-Martin, D., Szopa, S., Tyteca, S., Alkama, R., Belamari, S., Braun, A., Coquart, L. and Chauvin, F. (2013) The CNRM-CM5.1 global climate model: description and basic evaluation. *Climate Dynamics*, 40, 2091–2121. <https://doi.org/10.1007/s00382-011-1259-y>.
- Von Salzen, K., Scinocca, J.F., McFarlane, N.A., Cole, J.N.S., Plummer, D., Versegny, D., Reader, M.C., Ma, X., Lazare, M. and Solheim, L. (2013) The Canadian Fourth Generation Atmospheric Global Climate Model (CanAM4). Part I: physical processes. *Atmosphere–Ocean*, 51, 104–125. <https://doi.org/10.1080/07055900.2012.755610>.
- Wallace, J.M. and Gutzler, D.S. (1981) Teleconnection in the geopotential height field during the Northern Hemisphere winter. *Monthly Weather Review*, 109, 784–812.
- Watanabe, M., Suzuki, T., O’ishi, R., Komuro, Y., Watanabe, S., Emori, S., Takemura, T., Chikira, M., Ogura, T., Sekiguchi, M., Takata, K., Yamazaki, D., Yokohata, T., Nozawa, T., Hasumi, H., Tatebe, H. and Kimoto, M. (2010) Improved climate simulation by MIROC5: mean states, variability, and climate sensitivity. *Journal of Climate*, 23, 6312–6335.
- Weisheimer, A. and Palmer, T.N. (2014) On the reliability of seasonal climate forecasts. *Journal of the Royal Society Interface*, 11(96), 20131162. <https://doi.org/10.1098/rsif.2013.1162>.
- Winton, M. (2000) A reformulated three-layer sea ice model. *J. Atmos. Ocean. Tech.*, 17, 525–531.
- Wittenberg, A.T., Rosati, A., Lau, N.-C. and Ploshay, J.J. (2006) GFDL’s CM2 global coupled climate models. Part III: tropical Pacific climate and ENSO. *Journal of Climate*, 19, 698–722.
- Wu, T.W., Yu, R., Zhang, F., Wang, Z., Dong, M., Wang, L., Jin, X., Chen, D. and Li, L. (2010) The Beijing Climate Center atmospheric general circulation model: description and its performance for the present-day climate. *Climate Dynamics*, 34, 123–147.
- Wu, T.W., Li, W., Ji, J., Xin, X., Li, L., Wang, Z., Zhang, Y., Li, J., Zhang, F., Wei, M., Shi, X., Wu, F., Zhang, L., Chu, M., Jie, W., Liu, Y., Wang, F., Liu, X., Li, Q., Dong, M., Liang, X., Gao, Y. and Zhang, J. (2013) Global carbon budgets simulated by the Beijing Climate Center climate system model for the last century. *Journal of Geophysical Research*, 118, 4326–4347. <https://doi.org/10.1002/jgrd.50320>.
- Yang, X., Vecchi, G.A., Gudgel, R.G., Delworth, T. and Zhang, S. (2015) Seasonal predictability of extratropical storm tracks in GFDL’s high-resolution climate prediction model. *Journal of Climate*, 28, 3592–3611. <https://doi.org/10.1175/JCLI-D-14-00517.1>.
- Yin, Y., Alves, O. and Oke, P.R. (2011a) An ensemble ocean data assimilation system for seasonal prediction. *Monthly Weather Review*, 139, 786–808.
- Yin, Y., Alves, O. and Hudson, D. (2011b) Coupled ensemble initialization for a new intraseasonal forecast system using POAMA at the Bureau of Meteorology. In: *Proceedings of the International Union of Geodesy and Geophysics Conference (IUGG)*, 28 June–7 July, Melbourne, Australia.
- Zhang, S., Harrison, M.J., Rosati, A. and Wittenberg, A.T. (2007) System design and evaluation of coupled ensemble data assimilation for global oceanic climate studies. *Monthly Weather Review*, 135, 3541–3564. <https://doi.org/10.1175/MWR3466.1>.

How to cite this article: Scaife AA, Ferranti L, Alves O, *et al.* Tropical rainfall predictions from multiple seasonal forecast systems. *Int J Climatol.* 2019; 39:974–988. <https://doi.org/10.1002/joc.5855>